Title	Oxygen Solid Solution Strengthened Pure Titanium Powder Materials
Author(s)	Sun, Bin; Li, Shufeng; Imai, Hisashi et al.
Citation	Transactions of JWRI. 2012, 41(1), p. 59-64
Version Type	VoR
URL	https://doi.org/10.18910/23164
rights	
Note	

Oxygen Solid Solution Strengthened Pure Titanium Powder Materials[†]

SUN Bin*, LI Shufeng**, IMAI Hisashi**, UMEDA Junko***, KONDOH Katsuyoshi****

Abstract

The applications of Ti and its alloys are limited to high-performance products because of expensive cost and poor plastic formability. In order to develop a cost-effective processing route for pure Ti and its alloys, pure Ti powder was used as raw material and consolidated by different powder metallurgy routes in this study. Warm compaction and cold compaction were employed to consolidate Ti powder and spark plasma sintering (SPS) was used as reference method. The obtained compacts were subsequently hot extruded. The microstructure and mechanical properties of the hot-extruded pure Ti were evaluated. It was found that the samples prepared by warm compaction showed a higher tensile strength of 973.6 MPa, a better elongation of 26% and a higher hardness of 389.8 Hv comparing with the other two methods. Solid solution strengthening of oxygen was the main reinforcement mechanism for the sample prepared by warm compaction in this study. The strengthening effect of oxygen was calculated as 769.8 MPa / mass.%.

Key words: (powder metallurgy), (titanium), (spark plasma sintering), (solid solution), (reinforce)

1. Introduction

In recent years, weight reduction is one of the most effective methods to improve fuel consumption, and light metals are key materials in this regard. Ti has good specific properties such as low density of 4.51 g/cm^3, extremely high resistance for corrosion and great thermostability[1-6]. More and more attention has been paid for expanding the markets of Ti materials in aerospace and the automotive industry[7-10]. However, its mechanical properties are not good enough to employ for structural parts of mechanical products. On the other hand, Ti alloys such as Ti-6Al-4V alloy, one of the most conventional Ti alloys, is often applied for various fields of industries due to its high specific strength. However, the application is limited to high-performance products because of its low ductility and poor formability. In addition, high cost alloying elements such as V (vanadium) and difficulty with the melting process increase the total material cost of Ti-6Al-4V alloy. Therefore, alloy design, using low-price elements instead of rare metals such as V is strongly required.

Oxygen can dissolve in titanium to form an interstitial solid solution in a large amount (34 at.% in alpha titanium), it shows a strong hardness and mechanical strengthening on titanium matrix[1-3]. Therefore, instead of expensive rare metals such as vanadium (V), oxygen (O) is usually used as a attractive interstitial solid solution strengthening element. In this study, Powder Metallurgy Methods were applied to fabricate high strength Ti materials with oxygen solid solution, because they have lots of advantages[11-13]: 1) powder metallurgy technology can minimize the segregation of alloy components, eliminating bulky, uneven casting organization. 2) powder metallurgy technology can be used to prepare amorphous, microcrystalline, quasicrystals, nanocrystalline supersaturated solid solution and a series of high performance non-equilibrium materials. The most common Powder Metallurgy Method, warm compaction was applied to fabricate Ti materials, because warm compaction processing can produce the greatest benefits when coupled with high performance ferrous alloy compositions[14]. Since oxygen shows affinity with Ti during the heating process of warm compaction, a large amount of oxygen in the air will solve into Ti powder. In order to control solid solution of oxygen, spark plasma sintering (SPS) and cold compaction were also applied to consolidate pure Ti powder. Hot extrusion was employed to get full density materials. In order to evaluate the effect of grain refinement, before extrusion, heat treatment was applied to promote grain growth of Ti. The mechanical properties of extruded pure titanium powder material were evaluated. Mechanism of solid solution of oxygen and grain refinement was discussed.

2. Experimental

Pure Ti powder (99.5%, 25 µm) was used as the starting material. The SEM image is shown in **Fig. 1**. Four samples, Sample A, Sample B, Sample C and Sample D were prepared in this study. The flow chart of the experimental process was shown in **Fig. 2**. Sample A

---

was prepared by consolidating the raw powder by SPS system (DR.Sinter/SPS1030 system, Sumitomo Coal Mining) at 1073 K for 1.8 ks in a vacuum atmosphere with a pressure of 30 MPa. Sample B was prepared by compacting the raw powder at room temperature by a 2000 kN Hydraulic Press (HP) (SHP-200-450, Shibayama machine) and heating the compact at 673 K in a muffle furnace in argon atmosphere and compacting by HP. Sample C was prepared by heating the raw powder at 673 K in an argon atmosphere and compacting by HP. Then, the compacts of 42 mm in diameter were preheated in a muffle furnace at 1273 K for 180 s (Sample D : 1.8 ks) in argon gas, and immediately extruded at the extrusion ratio of 37, respectively. The extruded rods of 7 mm in diameter were obtained. Sample D was prepared by heating the raw powder at 673 K in an argon atmosphere and compacting by HP. Then, the sintered materials of 42 mm in diameter were heated at 1273 K for 1.8 ks in argon gas, and immediately extruded at the extrusion ratio of 37. The extruded rods of 7 mm in diameter were obtained.
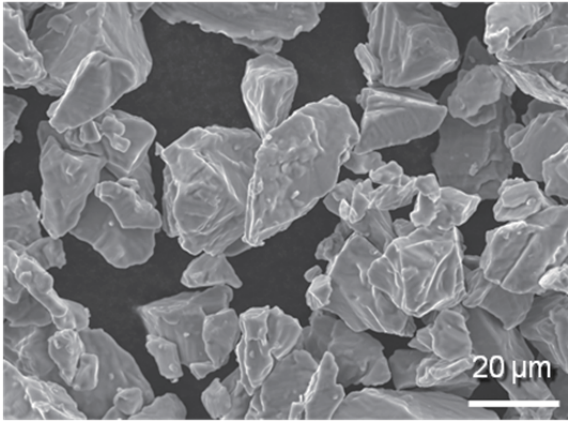
Fig. 1 SEM image of pure Ti powder.

The extruded samples for microstructure observation were prepared as follows; first, specimens were ground using emery paper of 4000 grit, and then, polished using alumina (Al_2O_3) fine particles suspension solution. Chemical etching treatment was carried out using the solution for titanium corrosion (H_2O: HF: HNO_3=100: 1: 5). The microstructure was observed using an optical microscope (OM) and scanning electrical microscope (SEM). The polished samples for electron back scattered diffraction (EBSD) analysis were prepared by electrolytic polishing at room temperature using the solution (acetic acid: 95%, perchloric acid: 5%) with a polishing time of 90 s. EBSD was carried out using a SEM equipped with an EBSD detector, operated at an acceleration voltage of 20 kV and a tilt angle of 70°. X-ray Diffraction (Labx, XRD-6100, Shimadazu) analysis was used to analyze lattice constants of different samples. The micro-hardness was measured by Vickers micro-hardness tester (HMV-2T; Shimadzu).

Mechanical properties of the extruded samples were evaluated by tensile test. Tensile test specimens, having a diameter of 3 mm and a gauge length of 20 mm, were machined from the extruded rods. Tensile tests were performed under a strain rate of 5×10^{-4} /s using a universal testing machine (Shimadzu Autograph AG-X 50 kN) at room temperature on four test specimens.

3. Results
3.1 Mechanical properties

The true strain-stress curves are shown in **Fig. 3**. Mechanical properties of each Ti sample are listed in table 1. It was observed that 0.2%YS, UTS and hardness of Sample C and D were much higher than that of Sample A and B. Especially, Sample C showed a good balance between strength and elongation. 0.2%YS of Sample C reached 832.8 MPa, and showed a 73% higher value than that of Sample A. In addition, elongation of Sample C remained at 26%, and showed the same level as Sample A. Furthermore, hardness of Sample C and Sample D were higher than that of Sample A and Sample B by about 100 Hv.

3.2 Reinforcement of grain refinement

Figure 4 shows optical microscope (OM) images of each extruded Ti sample. Grain sizes of Sample A, Sample B, Sample C and Sample D were measured and calculated as 12.32 μm, 10.09 μm, 9.32 μm and 12.43 μm, respectively. Sample A, prepared by SPS, was exposed at higher temperature of 1073 K for 30 min during the consolidation stage compared with sample B and sample C. Sample D, prepared by HP, was exposed at longer holding time of 1.8 ks during preheating of hot extrusion stage compared with sample C. As a result, grain sizes of sample A and sample D grew larger than those of other ones. The grain size effect on 0.2% YS is well known as the Hall-Petch relationship[15-18] through the following equation (1).
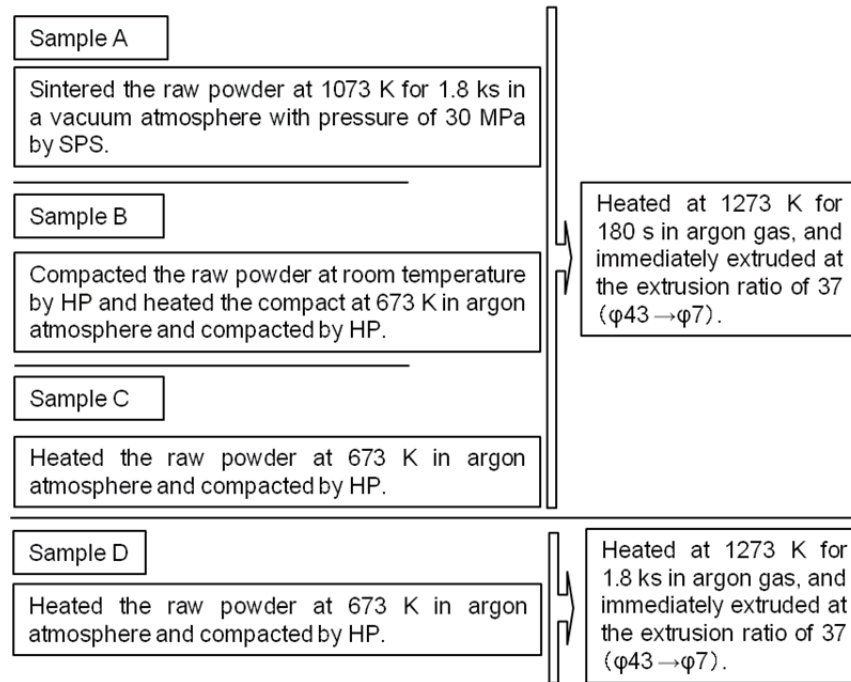
$$\sigma = \sigma_0 + kD^{-1/2} \tag{1}$$

σ_0 is a constant stress and k is a materials constant. D is a mean grain diameter of the Ti matrix. The constant stress σ_0 and the materials constant k for pure Ti matrix are reported as 172.5 MPa and 18 MPa/mm$^{-1/2}$[19]. Taking grain size of Sample D as standard, then, the grain refinement effect on 0.2% YS of Sample A, Sample B and Sample C was calculated as 5.4 MPa, 22.0 MPa and 23.2 MPa.
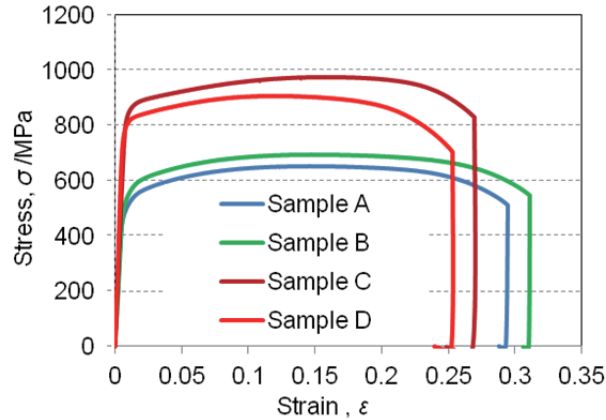
Figure 5 showed EBSD analysis result of each extruded Ti sample. The color code, red for <0001>, gave the crystallographic direction perpendicular to the extrusion direction, the green for <$2\bar{1}\bar{1}0$> and the blue for <$10\bar{1}0$>, gave the crystallographic direction Parallel to the extrusion direction. The same color code was used in the inverse pole figure, and naturally, the high intensity was found in the red region. Textured Ti demonstrates significantly different monotonic strength characteristics according to the direction of the principal stress relative to the predominant basal plane texture. Compared with the perpendicular direction, the transverse direction promotes a relatively high yield stress and UTS. The differences in mechanical behavior have been related to

the ability to induce slip in the various plate orientations[20]. In this study, extruded samples by different methods showed similar textures. The texture of

Ti after extrusion can be described as a texture with the <0001> direction perpendicular to the extrusion direction.

| Sample A |
| Sintered the raw powder at 1073 K for 1.8 ks in a vacuum atmosphere with pressure of 30 MPa by SPS. |

| Sample B |
| Compacted the raw powder at room temperature by HP and heated the compact at 673 K in argon atmosphere and compacted by HP. |

| Sample C |
| Heated the raw powder at 673 K in argon atmosphere and compacted by HP. |

Heated at 1273 K for 180 s in argon gas, and immediately extruded at the extrusion ratio of 37 (φ43 → φ7).

| Sample D |
| Heated the raw powder at 673 K in argon atmosphere and compacted by HP. |

Heated at 1273 K for 1.8 ks in argon gas, and immediately extruded at the extrusion ratio of 37 (φ43 → φ7).

Fig. 2 The flow chart of the experimental processes to prepare Sample A, B, C and D.
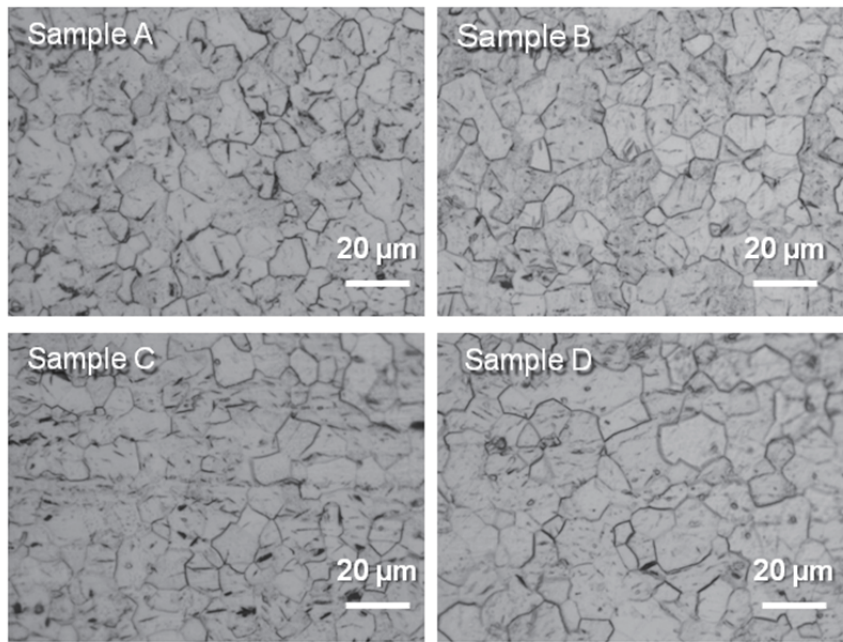

Fig. 3 Stress-strain curves of Sample A, B, C and D.

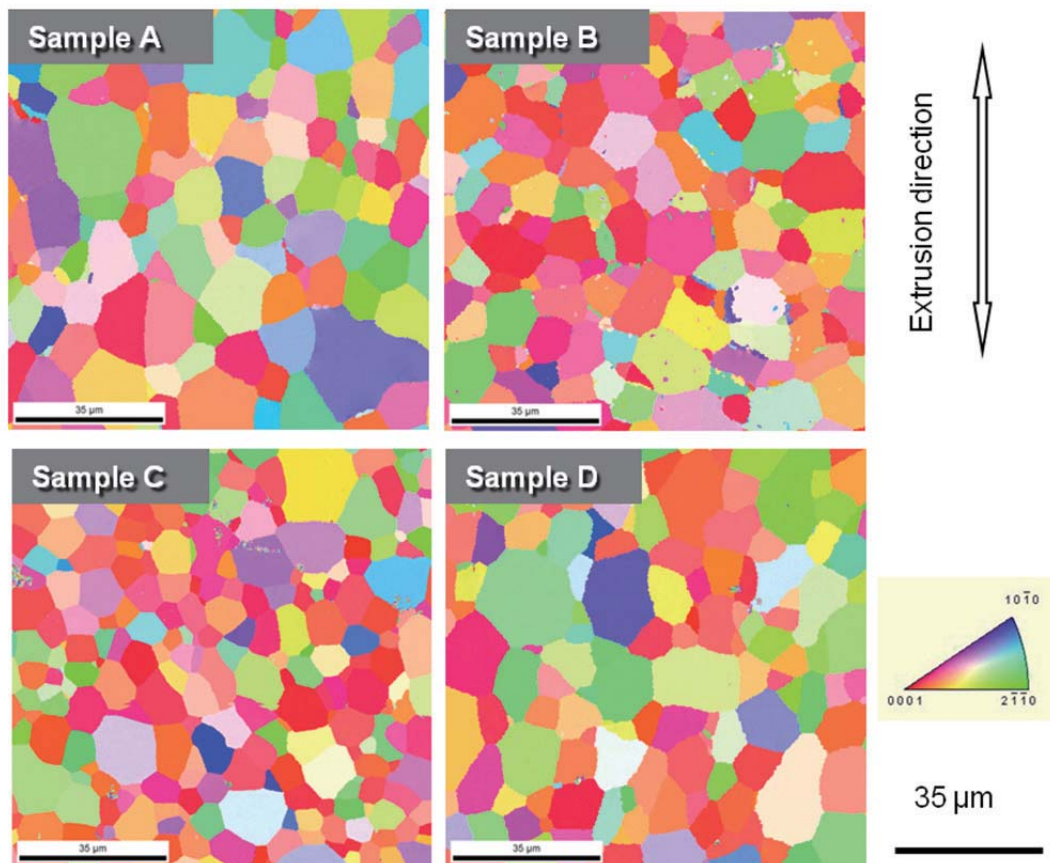**Table 1** Mechanical properties of Ti Sample A, B, C and D.

Sample Name	0.2%YS σ_y/ MPa	UTS σ/ MPa	Elongation ε (%)	Hardness H/ Hv$_{0.025}$
Sample A	479.2	622.2	28.7	264.8
Sample B	524.7	693.9	31.8	280.2
Sample C	832.8	973.7	26.0	389.8
Sample D	774.6	914.7	24.5	382.1

Fig. 4 Optical microscope images of the extruded Ti materials of Sample A, B, C and D.

Fig. 5 EBSD analysis results of extruded Ti materials of Sample A, B, C and D.

3.3 Reinforcement of solid solution of oxygen

XRD analysis results of the different samples are shown in **Fig. 6**. Ti lattice constants could be calculated from the Ti main peak shift. The distance of crystal plane d is expressed by Bragg's equation[21] as the following equation (2).

$$d = n \lambda / 2 \sin \theta \qquad (2)$$

Where n is positive integer, λ is X-ray wavelength, and θ is glancing angle. When the crystal structure is a hexagonal closed-packed lattice (hcp) such as Ti, magnesium (Mg) and zinc (Zn), d is also expressed as the following equation (3), h, k and l in the equation are the Miller indices.

$$d = 1 / \sqrt{4 \left(h^2 + k^2 + h\,k \right) / 3\, a^2 + l^2 / c^2} \qquad (3)$$

a and c are the lattice constants of a-axis and c-axis of hcp structure. The lattice constants are calculated by substituting the values of θ, h, k, l obtained from the result of XRD analysis in the equation 1 and 2. Lattice constant c of Sample C and Sample D increased large by compared with that of Sample A. Oxygen content of each sample was analyzed by ICP method (the model of the machine), and the results are listed in **Table 2**. By excluding the reinforcement effect of grain refinement, the reinforcement effect of solid solution of oxygen is shown in **Fig. 7**. The reinforcement effect of solid solution of oxygen was calculated as 769.8 MPa/mass%. In addition, hardness of Sample A, Sample B, Sample C and Sample D were measured as 264.8 Hv, 280.2 Hv, 389.8 Hv and 382.1 Hv. The micro-hardness of Ti based alloys was intensively enhanced by the diffusion of oxygen[22]. With the increased oxygen contents of the sample, hardness of the sample increased. The effect of solid solution of oxygen on hardness of Ti was calculated as 287.9 Hv/mass%.

4. Discussion

Low cost and mechanical properties comparable to those of wrought materials are two essential factors for structural use of P/M Ti and Ti alloys. Instead of rare metals such as vanadium (V), oxygen (O), nitrogen (N) and iron (Fe) are usually used as alloying elements to Ti and its alloys[23-26]. In particular, the maximum solid solubility of oxygen in alpha Ti is approximately 34 at.%[27,28], which is much larger than other conventional alloying elements. So, the large effects of oxygen for solid solution strengthening are expected. In the previous researches, Ti alloys were strengthened by solid solution of oxygen[29-31]. According to Qianqian Wei's research[29], Ti–Nb–Ta–Zr alloy with solid solution of oxygen was prepared by melted Ti–22.5Nb–0.7Ta–2Zr and TiO$_2$. However, the melting process of Ti alloy was applied for the fabrication of the alloy, and needs an immense amount of energy and special equipment, because of its high melting temperature and easy reactivity. As a result, the material cost became higher. In addition, grains of Ti alloys grew larger than 30 μm which will cause severe degradation of the mechanical properties. Powder Metallurgy Method was applied by T. Yoshimura's research[32], and Ti alloys were strengthened by TiO$_2$. They were mixed by ball mill for 7.2 ks, and then, sintered by SPS at 1073 K for 1.8ks. However, the process of the experiment took a long time, and the use of SPS increased the energy cost. In addition, the mechanism of solid solution of oxygen was not discussed. In this research, a PM titanium billet with good mechanical properties was prepared by warm compaction and hot extrusion process. During the process of warm compaction at 673 K, oxygen in the air solved into Ti powder, and strengthened the compact of Ti. After warm compaction and hot extrusion, 0.64 mass% oxygen solved into the crystal lattice of Ti. Compared with Sample A which was carried out by SPS, lattice parameter a of Sample C and Sample D did not vary apparently, however, the lattice parameter c of Sample C and Sample D increased from 4.689 Å to 4.695 Å and 4.696 Å. That is because Oxygen occupies the octahedral interstices in hcp metals. The strain induced by the interstitials in the crystal lattice along the Z-axis, perpendicular to the basal plane, is greater than that along the X- axes and Y-axes lying in the basal plane[33]. Lattice expansion due to foreign atoms in interstitial positions has been theoretically explained on the basis of the concept of elastic dipoles. The evaluation of mechanical properties of Sample C carried out by warm compaction showed a high tensile strength of 973.6 MPa, good elongation of 26% and high hardness of 389.8 Hv through solid solution of oxygen. The reinforcement effect of oxygen solid solution was calculated as 769.8 MPa/mass% on 0.2%YS and 287.9 Hv/mass% on hardness. Large energy and special equipment was not applied during the process of warm compaction and hot extrusion. As a result, energy and equipment costs became lower. In addition, since high temperature heat treatment was not carried out during the process, grains did not grow large, and strength and elongation did not decrease. Therefore, warm compaction and hot extrusion process is a good method for fabricating Ti composites for industry.
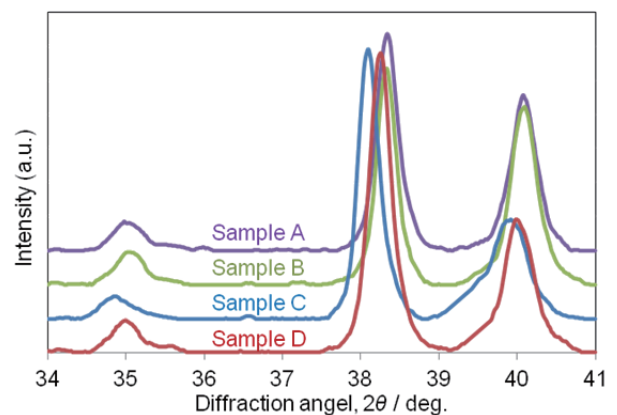
Fig. 6 X-ray diffraction patterns of extrude Ti Sample A, B, C and D.

Table 2 Lattice constants and oxygen content of Ti of Sample A, B, C and D.

Sample Name	a/ Å	c/ Å	O content (mass%)
Sample A	2.951	4.689	0.23
Sample B	2.953	4.690	0.26
Sample C	2.953	4.695	0.64
Sample D	2.953	4.696	0.64
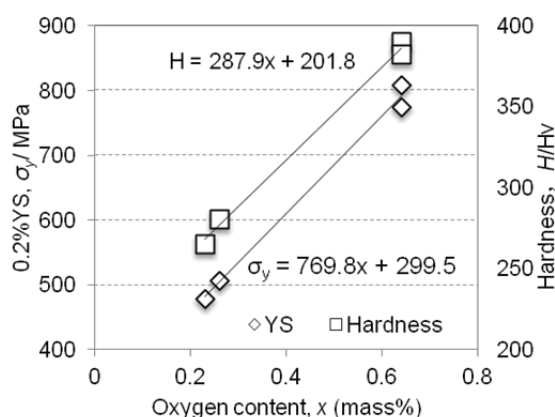
Fig. 7 Oxygen solid solution strengthening of P/M Ti samples.

5. Conclusions

The conclusions of the present study are as follows:

1) Pure Ti was used to fabricate the high-strength and low-cost Ti materials. The evaluation of mechanical properties at room temperature showed high tensile strength of 973.6 MPa, good elongation of 26% and high hardness of 389.8 Hv by warm compaction.

2) Oxygen solid solution was effective in improving the tensile properties of extruded HP-Ti material. The reinforcement effect of solid solution of oxygen was calculated as 769.8 MPa/mass% on 0.2%YS and 287.9 Hv/mass% on hardness.

3) Warm compaction and hot extrusion process was a good method to fabricate high strength pure Ti with low cost.

References

1) K. Okazaki, H. Conard, Transactions JIM. (1973) 14.
2) E. W. Collings, Materials properties Handbook, Titanium Alloys, Materials Park, OH, ASM International, 1994.
3) T. Yoshimura, T. Thotsaphon, H. Imai, K. Kondoh, Materials Science Forum. 654- 656.
4) M.P. Brady, W.J. Brindley, J.L. Smialek, Journal of Metals. 48 (1996) 46-50.
5) Y.L. Xi, D.L. Chai, W.X. Zhang, J.E. Zhou, Scripta Materialia. 54 (2006) 19-23.
6) J.R.B. Gilbert, Materials Science and Technology. 1 (1985) 257-262(6).
7) F.H. Froes, H. Friedrich, J. Kiese, D. Bergoint, JOM. 56 (2004) 40.
8) O. Schauerte, Advanced Engineering Materials. 5 (2003) 411–418.
9) F.J. Hideki, T.H. Kazuhiro, Y.S. Yoshito, Nippon Steel Tecnical Report. 88 (2003).
10) K. Faller, F.H. Froes, JOM. 53 (2001) 27.
11) K.S. Narasimhan, Advantage Performance Materails. 3-1 (1996) 7-27.
12) J.R. Pickens, Journal of the Society of Materials Science. 16-6 (1981) 1437-1457.
13) Y. Liu, L.F. Chen, H.P. Tang, C.T. Liu, B. Liu, B.Y. Huang, Materials Science and Engineering A. 418 (2006) 25–35.
14) Z. Howard, H. Francs, International Conference on Powder Metallurgy & Particulate Materials. 1997 6.27-7.2.
15) C. Mercer, W. O. Soboyejo, Scripta Materialia. 35-1 (1996) 17-22.
16) T. Jiancheng , H. Baiyun, H. Yuehui , L. Wensheng , Z. Kechao , W. Aihua, Materials Research Bulletin. 37-7 (2002) 1315-1321.
17) E.O. Hall, Proceedings of the Physical Society. 64B (1951) 747.
18) N.J. Petch, The Journal of the Iron and Steel Institute. 173 (1953) 25.
19) Y. Kobayashi, Y. Tanaka and K. Matsuoka: Society of Materials Science, Japan. 54 (2005) 66-72.
20) M.R. Bache, W.J. Evans, Materials Science and Engineering A. 319–321 (2001) 409–414.
21) W.L. Bragg, Cornell University Press, Ithaca, New York, 1937.
22) M. Hongyan, W. Maocai, Z. Song, X. Gongchun, W Zheng, Transactions Nonferrous Materials Society, China. 13-1 (2003) 52.
23) A.E. Jenkins and H.W. Worner, Journal of the Institute of Metals. 80 (1951-52) 157-166.
24) O. Yamamoto, K. Alvarez, T. Kikuchi and M. Fukuda, Acta Biomaterialia. 5 (2009) 3605-3615.
25) T. Ando, K. Nakashima, T. Tsuchiyama and S. Takai, Materials Science and Engineering A. 486 (2008) 228-234.
26) M. Koike, C. Ohkubo, H. Sato, H. Fujii and T. Okabe, Materials Science and Engineering C. 25 (2005) 349-356.
27) H. Conrad, Progress in Materials Science. 26 (1981) 123-403.
28) J. Unnam, R.N. Shenoy and R.K. Clark, Chemstry and Material Science. 26 (1986) 231-252.
29) Q. Wei, L. Wang, Y. Fu, J. Qin, W. Lu and D. Zhang, Materials and Design. 32 (2011) 2934-2939.
30) D.J. Simbi and J.C. Scully, Materials Letters. 26 (1996) 35-39.
31) F. Geng, M. Niinomi, M. Nakai, Materials Science and Engineering A. 528 (2011) 5435-5445.
32) T. Yoshimura, T. Thotsaphon, H. Imai, K. Kondoh, Transactions of JWRI, 38(2009) 2.
33) M.S. Blanter, E.B. Granovskiy, L.B. Magalas, Mater Science Engineering A 370(2004) 88–92.